COMM. MATH. SCI.
Vol. 1, No. 1, pp. 30–43

MODELING 2D AND 3D HORIZONTAL WELLS USING CVFA*

ZHANGXIN CHEN, GUANREN HUAN, AND BAOYAN LI†

Abstract. In this paper we present an application of the recently developed control volume function approximation (CVFA) method to the modeling and simulation of 2D and 3D horizontal wells in petroleum reservoirs. The base grid for this method is based on a Voronoi grid. One of the features of the CVFA is that the flux at the interfaces of control volumes can be accurately computed via function approximations. Also, it reduces grid orientation effects and applies to any shape of elements. It is particularly suitable for hybrid grid reservoir simulations. Through extensive numerical experiments and comparisons with the finite difference method for benchmark flow problems, we show that this method can efficiently and accurately handle complex horizontal wells in any direction.

Key words. reservoir simulator, horizontal well in any direction, finite difference, control volume function approximation, numerical experiments

AMS subject classifications. 35K60, 35K65, 76S05, 76T05

1. Introduction

Recent interest in the modeling and numerical simulation of horizontal wells in petroleum reservoirs has rapidly increased because of improved drilling technology [14]. The use of horizontal wells not only leads to the increased efficiency and economy of oil recovery operations, also it decreases the coning behavior with an increase in well length and enlarges oil-sweeping volumes. For gas reservoirs with low permeability, it decreases turbulence effects at gas wells and increases production rates.

The finite difference (FD) method has been widely used in the numerical simulation of fluid flow in petroleum reservoirs [1, 16]. However, due to the structure of rectangular grids it uses, this method can model horizontal wells only in coordinate directions. Also, this method causes numerical dispersion and grid orientation problems and possesses difficulties in the treatment of complicated geometry and boundary conditions. On the other hand, one has tried to utilize the intrinsic grid flexibility of the finite element method [5], but this method does not conserve mass locally [2]. Recently, the control volume finite element (CVFE) method has been developed to enforce such a conservation property [9], but it often produces inaccurate fluid velocities and cannot easily generate the streamlines of fluid flow in reservoir simulations. The reason is that the usual CVFE method uses linear elements to present pressure, and it leads to a piecewise constant velocity. Although the flux across the interior boundaries of control volumes is forced to be continuous in an *ad hoc* manner in [18], the approach involved is not physical.

This paper presents an application of the recently developed control volume function approximation (CVFA) method [12, 13] to the modeling and numerical simulation of 2D and 3D horizontal wells in petroleum reservoirs. This CVFA method is more accurate in the approximation of both pressure and velocity in the simulation of multiphase flow in reservoirs, locally conserves mass, has less grid orientation effects, and applies to any shape of elements. It is particularly suitable for hybrid grid reservoir

*Received: February 15, 2002; Accepted (in revised version): May 11, 2002.

†Department of Mathematics, Box 750156, Southern Methodist University, Dallas, TX 75275-0156 (zchen@mail.smu.edu), (huan@golem.math.smu.edu), (bli@mail.smu.edu). This work is supported in part by National Science Foundation grants DMS-9972147 and INT-9901498 and by a gift grant from the Mobil Technology Company.

simulations. In this paper we employ it to model and simulate 2D and 3D horizontal wells in any direction. Extensive numerical experiments, together with comparisons with the FD method for benchmark two-phase flow problems, show that the CFVA is accurate and reliable in modeling and simulating these wells.

This paper is organized as follows. In the next section we introduce the grids on which the CVFA method is based. Then, in the third section we briefly review the CVFA and its recent applications. In the fourth section, we describe a two-phase flow model, present the application of the CVFA to the modeling of 2D horizontal wells, and compare it with the FD method. In the fifth section we extend it to the application of 3D horizontal wells. Concluding remarks are given in the last section.

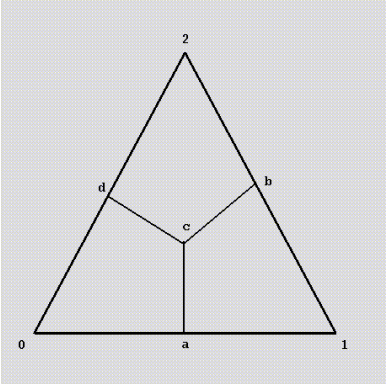

FIG. 1. *A triangle into smaller triangles.*

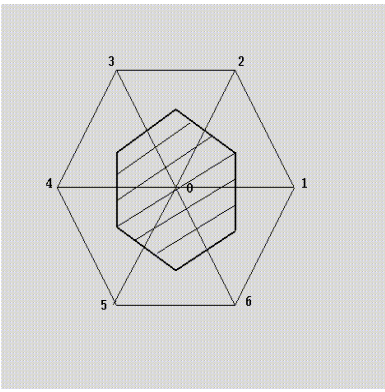

FIG. 2. *A control volume.*

2. Grids

In this section we introduce the grids on which the CVFA method is based, i.e., the Voronoi grids. These grids, also called PEBI (perpendicular bisection) grids, were introduced by Heinrich in 1987 [11] in two dimensions. These grids are locally orthogonal; i.e., the block boundaries are normal to lines joining the nodes on the two sides of each boundary. This allows a reasonably accurate approximation of interblock transmissibility for heterogeneous but isotropic permeability distribution. There are extensions of the Voronoi grids where anisotropic permeability tensors can be handled and the grid block boundaries are not locally orthogonal [10, 15, 18]. In this paper, as an example, we construct the Voronoi grids from triangles [18].

The base grid of a reservoir consists of triangles. Then each triangle is divided into six smaller triangles by connecting its center with the midpoints on its three edges (see FIG. 1), and a control volume consists of all smaller triangles sharing the same vertex of a large triangle (see FIG. 2), which is the center of this control volume. (We remark that while it is in 2D, we still call it a "volume" as usual [10, 15, 18].) Now, a Voronoi grid is composed of all control volumes. A control volume near the boundary of the reservoir consists of fewer triangles. Control volumes should have equal sides to reduce grid orientation effects. The Voronoi grid constructed in this way has many advantages. First, it can effectively reduce grid orientation effects. Second, it can easily be adapted for local grid refinement. Third, it allows for an easy and accurate treatment of faults, corner points, and cracks.

In this paper, as three-dimensional grids, stacks of the two-dimensional Voronoi grids are used to model vertical variation in reservoir properties, and thus the grids

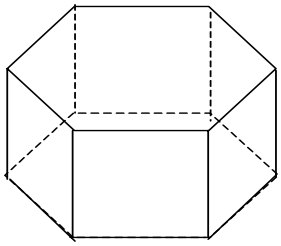

FIG. 3. *A 3D control volume.*

in the vertical direction are of cylindrical type (see FIG. 3). This approach simplifies the computation of fluid flow between different vertical layers.

3. The CVFA Method

In this section we very briefly review the CVFA method. For more information about this method, the reader may refer to [12, 13].

We consider a typical flow equation in 2D for the unknown Φ:

$$\frac{\partial}{\partial t}(\phi\Phi) = \nabla \cdot (\mathbf{K}\nabla\Phi) + q, \tag{3.1}$$

where ϕ and $\mathbf{K}$ are given functions and q is a sum of source/sink terms. The fluid velocity can be defined as $\mathbf{u} = -\mathbf{K}\nabla\Phi$, so equation (3.1) is rewritten as

$$\frac{\partial}{\partial t}(\phi\Phi) = -\nabla \cdot \mathbf{u} + q. \tag{3.2}$$

For a given control volume V in plane with surface A, after an application of the divergence theorem the integral form of (3.2) is

$$\int_V \frac{\partial}{\partial t}(\phi\Phi)\ dV = -\int_A \mathbf{u}\cdot\mathbf{n}\ dA + \int_V q\ dV, \tag{3.3}$$

where $\mathbf{n}$ is the outer unit normal to A. On V, an interpolant Φ^I is used to approximate Φ:

$$\Phi^I(\mathbf{x}, t) = \sum_{j=1}^{M} \Phi_j(t)\varphi_j(\mathbf{x}), \quad \mathbf{x} \in V, \tag{3.4}$$

where M is the number of the interpolation functions associated with V. We have used different approximation functions as the interpolation functions such as spline, weighted distance, and "bilinear" functions [12, 13]. As an example, we briefly sketch a bilinear approach to see the difference between the CVFA and CVFE.

Let points $0, 1, \ldots, 5$ be vertices of triangles (see FIG. 4). They are centers of control volumes. In the CVFE [8, 9, 18], the velocity $\mathbf{u}$ at the interface ac is calculated via a linear polynomial interpolation which involves the values of Φ at points 0, 1, and 2. In fact, the calculation of $\mathbf{u}$ at all interfaces ac, bc, and dc involves only points 0, 1, and 2. In contrast, in the CVFA the calculation of $\mathbf{u}$ at ac involves the values of Φ at points 0, 1, 2, and 3. Similarly, the calculation of $\mathbf{u}$ at bc and dc involves 0, 1, 2, and 4, and 0, 1, 2, and 5, respectively. Since the CVFA uses a higher order interpolation, the calculation of $\mathbf{u}$ is more accurate than that in the CVFE.

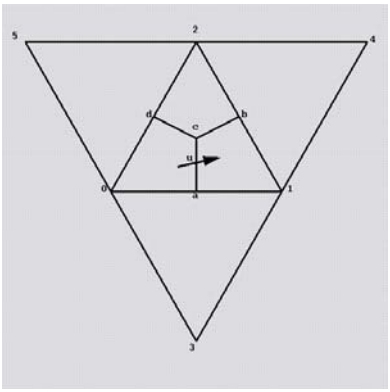

FIG. 4. *Interpolation points.*

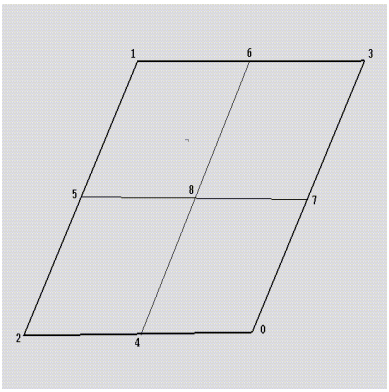

FIG. 5. *The bilinear interpolation.*

We define the interpolation basis functions in the present case. Let points 0, 1, 2 and 3 be the centers of four control volumes (see FIG. 5). To interpolate the value of Φ at point 8 on a control-volume interface, we employ expression (3.4), i.e.,

$$\Phi_8 = \Phi_0\varphi_0 + \Phi_1\varphi_1 + \Phi_2\varphi_2 + \Phi_3\varphi_3. \tag{3.5}$$

Let 4, 5, 6, and 7 be the projection points of 8 on the four edges according to the distance rule

$$\frac{R_{42}}{R_{02}} = \frac{R_{61}}{R_{31}} = \frac{R_{85}}{R_{75}}, \quad \frac{R_{52}}{R_{12}} = \frac{R_{70}}{R_{30}} = \frac{R_{84}}{R_{64}},$$

where R_{ij} indicates the distance between points i and j. The "bilinear" interpolation takes the form

$$\begin{aligned} \Phi_8 &= \Phi_5 + (\Phi_7 - \Phi_5)\frac{R_{85}}{R_{75}}, \\ \Phi_5 &= \Phi_2 + (\Phi_1 - \Phi_2)\frac{R_{52}}{R_{12}}, \\ \Phi_7 &= \Phi_0 + (\Phi_3 - \Phi_0)\frac{R_{70}}{R_{30}}. \end{aligned} \tag{3.6}$$

Substituting the second and third equations into the first equation in (3.6), we see that

$$\begin{aligned} \varphi_0 &= \left(1 - \frac{R_{70}}{R_{30}}\right)\frac{R_{85}}{R_{75}}, & \varphi_1 &= \frac{R_{52}}{R_{12}}\left(1 - \frac{R_{85}}{R_{75}}\right), \\ \varphi_2 &= \left(1 - \frac{R_{52}}{R_{12}}\right)\left(1 - \frac{R_{85}}{R_{75}}\right), & \varphi_3 &= \frac{R_{70}}{R_{30}}\frac{R_{85}}{R_{75}}. \end{aligned}$$

Note that these functions are defined in terms of distances and look like bilinear functions in form. That is why we have quoted "bilinear."

For a 3D problem, the grid to be used consists of elements as in FIG. 3, and accordingly the numerical procedure is based on the CVFA in the horizontal direction and a block-centered finite difference in the vertical direction. As noted, this approach simplifies the computation of fluid flow between different vertical layers.

The CVFA method has been applied to the following areas:

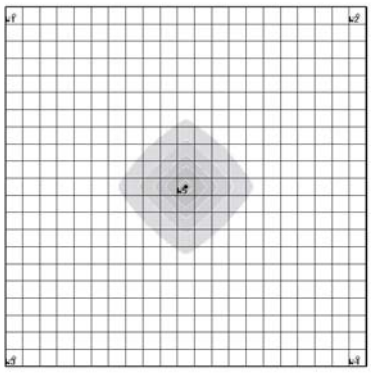

FIG. 6. *An example on rectangular grids.*

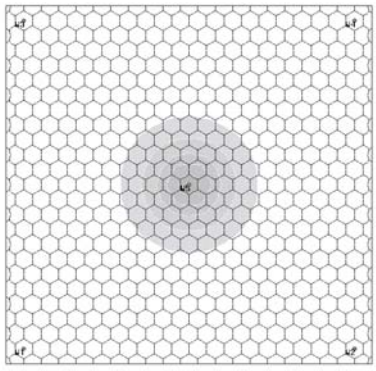

FIG. 7. *An example on Voronoi grids.*

3.1. Grid Orientation Effects. A major problem that has plagued the simulation of fluid flow in reservoirs is the grid-orientation effect [1, 7]. It is well understood that the FD method is sensitive to grid directions. A numerical example using the five-point FD method for a waterflooding problem (see the next section) is shown in FIG. 6, where the water saturation is shown. In this problem an injection well sits at the center of the domain, and four production wells are located at the four corners. From this figure we clearly see the grid orientation effect; water flows faster along the horizontal and vertical directions than along the diagonal directions. For the same problem, a numerical example using the CVFA over a Voronoi grid is displayed in FIG. 7. ¿From this figure we see that the orientation effect is gone.

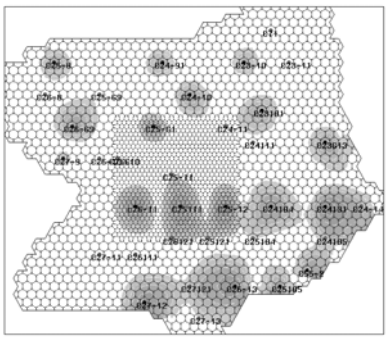

FIG. 8. A local refinement.

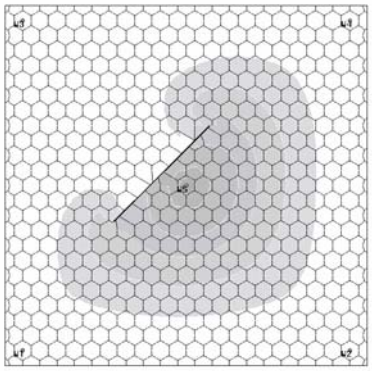

FIG. 9. A typical fault.

3.2. Local Grid Refinement. The use of triangles in the base grid to generate a Voronoi grid makes it easy to do local grid refinement. As noted, a triangle can be divided into smaller triangles by connecting its center with the midpoints on its three edges, and new (smaller) control volumes can be generated from the smaller triangles. A numerical example based on a local refinement is illustrated in FIG. 8 for a water flooding problem with 35 wells.

3.3. The Treatment of Faults. The transmissibility between two points across

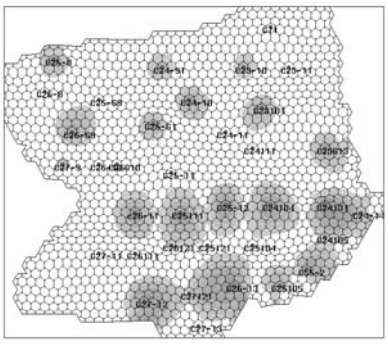

FIG. 10. *A CP technique.*

a fault in a control volume is set to be zero. This approach is easy to implement and is practical. A numerical experiment is shown in FIG. 9.

3.4. A Corner Point Technique. A corner point (CP) technique has been used in the FD method to adjust the location of vertical wells [6]. When the location of these wells is not at the centers of rectangles in the FD, there would be a significant error if the CP technique was not used. The CP technique in the FD is to adjust the four vertices of a rectangle. For the Voronoi grid under consideration, we exploit a similar technique to adjust the centers of control volumes. A numerical example using the CP technique is shown in FIG. 10.

4. Horizontal Wells and 2D Numerical Tests

In the previous section we have reviewed the recent applications of the CVFA. The purpose of this paper is to introduce its application to the treatment of horizontal wells in any direction (i.e., slanted wells).

4.1. Two-Phase Flow. For the flow of two immiscible fluids in a reservoir $\Omega \subset \Re^d$ $(d \leq 3)$, the mass balance equation for each of the fluid phases is

$$\phi \frac{\partial(\rho_\alpha s_\alpha)}{\partial t} + \nabla \cdot (\rho_\alpha \mathbf{u}_\alpha) = \rho_\alpha q_\alpha, \quad \alpha = w, o, \tag{4.1}$$

where $\alpha = w$ denotes the wetting phase (e.g., water), $\alpha = o$ indicates the nonwetting phase (e.g., oil), ϕ is the porosity of the medium, and ρ_α, s_α, $\mathbf{u}_\alpha$, and q_α are, respectively, the density, saturation, volumetric velocity, and external volumetric flow rate of the α-phase. The volumetric velocity $\mathbf{u}_\alpha$ is given by the Darcy law

$$\mathbf{u}_\alpha = -\frac{K_{r\alpha}}{\mu_\alpha}\mathbf{K}\nabla(p_\alpha - \rho_\alpha g Z), \quad \alpha = w, o, \tag{4.2}$$

where $\mathbf{K}$ is the absolute permeability of the porous medium, p_α, μ_α, and $K_{r\alpha}$ are the pressure, viscosity, and relative permeability of the α-phase, respectively, g denotes the gravitational constant, Z is the depth, and the z-coordinate is in the vertical downward direction. In addition to (4.1) and (4.2), the customary property for the saturations is

$$s_w + s_o = 1, \tag{4.3}$$

and the two pressures are related by the capillary pressure function

$$p_c(s_w) = p_o - p_w. \tag{4.4}$$

Following [17], q_w and q_o at a well can be defined by

$$\begin{aligned} q_w &= PI\frac{K_{rw}}{\mu_w}\big(p_{BH} - p_w - \rho_w g(Z_{BH} - Z)\big), \\ q_o &= PI\frac{K_{ro}}{\mu_o}\big(p_{BH} - p_o - \rho_o g(Z_{BH} - Z)\big), \end{aligned} \tag{4.5}$$

where PI is the productivity index of this well and p_{BH} is the flowing bottom hole pressure at the datum level depth Z_{BH}. The productivity index PI is given by

$$PI = \frac{2\pi\bar{K}h}{\ln\dfrac{r_e}{r_c}},$$

where the quantity $\bar{K}$ is some average of $\mathbf{K}$ at the well, h is the depth of this well, r_e is the equivalent radius, and r_c is the radius of this well. The definition of $\bar{K}$ and r_e is crucial, which will be discussed in the subsequent subsections.

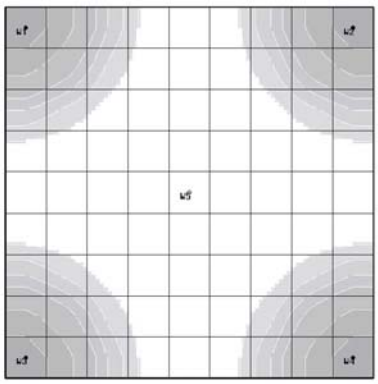

FIG. 11. *The saturation by FD.*

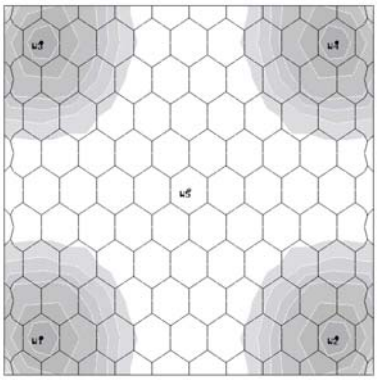

FIG. 12. *The saturation by CVFA.*

4.2. Vertical Wells. Before we treat horizontal wells, we first introduce an approach to model vertical wells. In the standard FD method, for a diagonal tensor $\mathbf{K} = \mathrm{diag}(K_{11}, K_{11}, K_{33})$ and a vertical well, $\bar{K}$ and r_e are defined as [17]

$$\bar{K} = K_{11}, \quad r_e = 0.14\left(DX^2 + DY^2\right)^{1/2}, \tag{4.6}$$

where K_{11} and K_{33} are the permeabilities in the horizontal and vertical directions, respectively, and DX and DY are the x and y dimensions of the grid block which contains this vertical well.

For the CVFA method, $\bar{K}$ is defined as in (4.6), and we calculate r_e by

$$r_e = \sqrt{\frac{A}{\pi}}, \tag{4.7}$$

where A is the area of a control volume V in the horizontal direction which contains this well. The derivation of (4.7) is based on the following observations: A is treated

as the area of a circle with radius r_e and the mean value of pressure on V is treated as the pressure over the surface of this circle. We have done many numerical experiments to check the correctness and accuracy of (4.7). Below we present one of them.

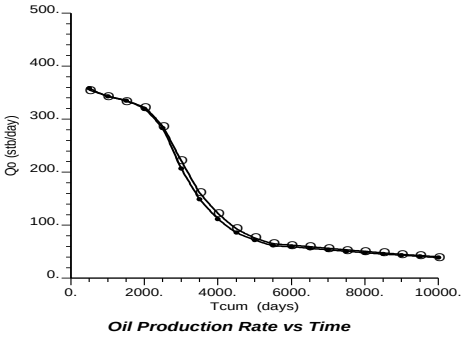

FIG. 13. $\circ$=*FD and* $\bullet$=*CVFA.*

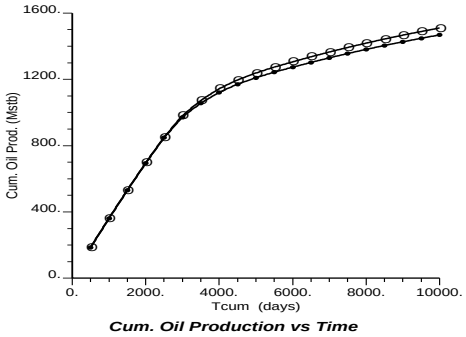

FIG. 14. $\circ$=*FD and* $\bullet$=*CVFA.*

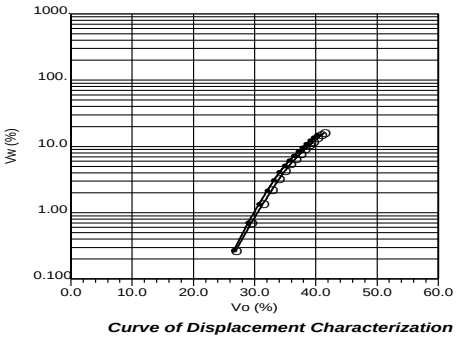

FIG. 15. $\circ$=*FD and* $\bullet$=*CVFA.*

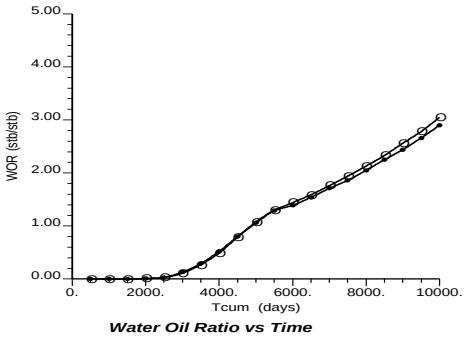

FIG. 16. $\circ$=*FD and* $\bullet$=*CVFA.*

The model problem is a five-spot pattern, waterflooding problem with four injectors at the four corners of a rectangular reservoir and a producer at the center of this reservoir. The porosity is $\phi = 0.2$, $K_{11} = 300$ md, and the reservoir dimensions are $1,000 \times 1,000 \times 100$ ft^3 (the flow is two dimensional; i.e., it is uniform in the z direction and the gravity is ignored). The bottom hole pressures at injection and production wells are $3,700$ psi and $3,500$ psi, and the water and oil viscosities are 0.4 cp and 6.0 cp, respectively. The relative permeability data are given in Table 1, and the capillary pressure is zero. No flow boundary conditions are used in this example.

Table 1. The relative permeability data.

s	0.22	0.3	0.4	0.5	0.6	0.8	0.9	1
K_{rw}	0	0.07	0.15	0.24	0.33	0.65	0.83	1
K_{ro}	1	0.4	0.125	0.0649	0.0048	0	0	0

We compare numerical results produced by the CVFA and those by the nine-point FD method, which exploits (4.6) to model wells. It is well known that the

nine-point FD method is more accurate than the five-point FD method and has less grid orientation effects.

An improved IMPES (implicit pressure-explicit saturation) method [3] is used to solve the two-phase system in the previous subsection. This system is written in terms of a pressure (the oil pressure) and a saturation (the water saturation). This improved IMPES method utilizes an adaptive control strategy on the choice of a time step for the saturation and takes a much larger time step for pressure than for the saturation. It has been shown [3] that it is effective and efficient for the numerical simulation of two-phase flow and it is capable of solving two-phase coning problems.

The saturation profile at $1,500$ days by the FD and CVFA is presented, respectively, in FIGS. 11 and 12. Also, for a comparison, the daily oil production rate (stb/day) versus time (days), the cumulative oil production (Mstb), the characterization curve of displacement (frac), and the water and oil production ratio (stb/stb) by these two methods are shown in FIG. 13–16. From these figures we see that these four curves match quite well. This shows the correctness and accuracy of (4.7). In many numerical experiments we have carried out, if the productivity index PI is not accurately calculated, there would be a significant amount of errors in these four curves.

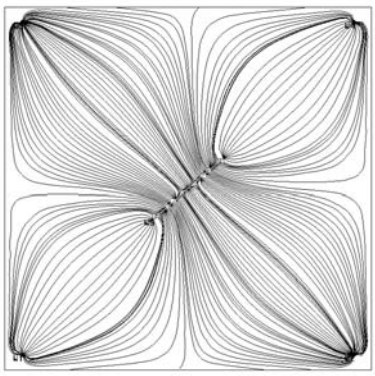

FIG. 17. *A streamline map.*

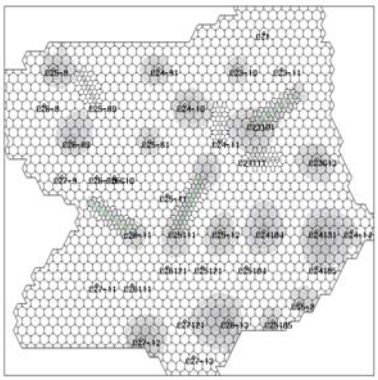

FIG. 18. *An example with multiple horizontal wells.*

4.3. Horizontal Wells. In the standard FD method, for a diagonal tensor $\mathbf{K} = \mathrm{diag}\,(K_{11}, K_{11}, K_{33})$ and a horizontal well (e.g., in the x direction), $\bar{K}$ and r_e are determined by [17]

$$\bar{K} = \sqrt{K_{11}K_{33}}, \quad r_e = \frac{0.14\left(\left(\frac{K_{33}}{K_{11}}\right)^{1/2} DX^2 + \left(\frac{K_{11}}{K_{33}}\right)^{1/2} DZ^2\right)^{1/2}}{0.5\left(\left(\frac{K_{33}}{K_{11}}\right)^{1/4} + \left(\frac{K_{11}}{K_{33}}\right)^{1/4}\right)}, \tag{4.8}$$

where DZ is the z dimension of the grid block containing this horizontal well.

For the CVFA method, $\bar{K}$ is defined as in (4.8), and we compute r_e in the following approach: Let a control volume V in the horizontal direction contain part of this horizontal well and L be the diameter of this volume in the well direction; then we

calculate r_e by

$$r_e = \sqrt{\frac{A\ DZ}{L\pi}}, \tag{4.9}$$

where we recall that A is the area of V and DZ is as in (4.8). The derivation of (4.9) is based on a similar principle as for (4.7). Again, we have done many numerical experiments to check the correctness and accuracy of (4.9). The comparison between the FD and CVFA with horizontal wells will be presented in the next section for 3D flow problems. In the rest of this section, we apply (4.9) to a couple of 2D numerical tests, which cannot easily be done using the FD.

The first numerical test uses the same physical and fluid data as in the previous subsection except that now the producer in the center of the reservoir is a horizontal well in 45°. In this test, instead of a saturation map, a streamline map is shown in FIG. 17. It is understood that these streamlines are very important in understanding the essentials of oil recovery processes. In the second test there are 35 wells, and six of them are horizontal wells in various directions. The saturation profile for this test is shown in FIG. 18. These two tests indicate that horizontal wells in different directions can be accurately and efficiently modeled using the CVFA method.

Table 2. The bottom hole pressure p_{BH} (psia).

Cases	1a	1b	2a	2b	3a	3b
Producer	3,513.6	3,506.44	3,389.43	3,529.9	3,270.0	3,472.0
Injector	3,651.4	3,651.4	3,651.4	3,651.4	3,651.4	3,651.4

Table 3. The relative permeabilities and capillary pressure for a water/oil system.

s_w	0.22	0.3	0.4	0.5	0.6	0.8	0.9	1
K_{rw}	0	0.07	0.15	0.24	0.33	0.65	0.83	1
K_{ro}	1	0.4	0.125	0.0649	0.0048	0	0	0
p_c	6.3	3.6	2.7	2.25	1.8	0.9	0.45	0.0

5. 3D Numerical Tests

We now perform numerical tests for a 3D problem which is concerned with the effect of horizontal well lengths and rates on oil recovery. This problem involves injection and production from horizontal wells in a reservoir where a coning tendency is important. The physical data for the reservoir and fluids are taken from [14] for a benchmark three-dimensional, three-phase black oil model. In this section we simplify this model by reducing from three phases to two phases and from a compressible case to an incompressible case. Recently, we have performed a comparison between the three and two phases and between the compressible and incompressible cases [4], and found that the effects of well lengths and rates on recovery are similar, and so is the behavior of daily oil production rates, cumulative oil production, and water-oil ratios. Moreover, it has been observed that the incompressible case is a very reasonable approximation of the compressible case, and thus the incompressible case can be used for numerical simulation tests in place of the compressible case.

The problem considered deals with oil recovery by bottom water drive in a reservoir. Fluids are produced from a horizontal well drilled in the top layer (Layer one). This well passes through the grid block centers and the entire length is open to flow.

Table 4. The physical and fluid data.

Item	Unit	Data
Dimensions $NX \times NY \times NZ$		$9 \times 9 \times 6$
Grid size DX	ft	$9 * 300$
Grid size DY	ft	620 400 200 100 60 100 200 400 620
Grid size DZ	ft	20 20 20 20 30 50
Depth of grid centers in z	ft	3600 3620 3640 3660 3685 3725
Initial water saturation in z	frac	0.289 0.348 0.473 0.649 0.869 1.00
Porosity	frac	0.2
Horizontal permeability	md	300
Vertical permeability	md	30
Water density	g/cm^3	0.9814
Water viscosity	cp	0.96
Water formation factor	rb/stb	1.0142
Oil density	g/cm^3	0.8975
Oil viscosity	cp	0.954
Oil formation factor	rb/stb	1.11
Radius of wellbore	inches	2.25
Time step for calculation	days	100
Ultimate time for calculation	days	1,500
Length of oil horizontal well	ft	900 (for cases 1a, 2a, 3a)
Length of oil horizontal well	ft	2,100 (for cases 1b, 2b, 3b)
Length of water horizontal well	ft	2,700 (for all cases)
Layer of oil horizontal well		1
Layer of water horizontal well		6
Grids of horizontal wells in y		5 (for all cases)
Grids of oil well in x		6-8 (for cases 1a, 2a, 3a)
Grids of oil well in x		2-8 (for cases 1b, 2b, 3b)

Two lengths are presented: (a) $\ell = 900$ ft and the well is stretched in grid blocks $(i, 5, 1)$, $i = 6, 7, 8$; (b) $\ell = 2,100$ ft and the well is stretched in grid blocks $(i, 5, 1)$, $i = 2, 3, \ldots, 8$. The flow direction in this well is from left to right, and the fluids are removed from the portion of this well in grid block (8,5,1) to the surface.

A constant pressure line source is exploited to simulate the bottom water drive. This line source is stretched in grid blocks $(i, 5, 6)$, $i = 1, 3, \ldots, 9$. A fixed pressure condition is also utilized at the production well, and six cases are considered as in Table 2, where the datum level depth Z_{BH} is 3,600 ft. Case a corresponds to $\ell = 900$ ft and case b to $\ell = 2,100$ ft. Other data are described in Tables 3 and 4.

We compare the daily oil production rates, cumulative oil production, and water-oil ratios by the CVFA with those by the FD. The CVFA treats the horizontal wells via (4.9), while the FD treats them via (4.8). The comparison for cases 1 and 3 is illustrated in FIG. 19–24, where $\bullet$ indicates the CVFA and $\circ$ the FD. These figures show that the numerical results by these two approximation methods match very well. Again, this shows the correctness, accuracy, and reliability of (4.9).

We now use the CVFA to compare the six cases in Table 2. The daily oil production rates between cases 1a, 2a, and 3a and between cases 1b, 2b, and 3b are displayed, respectively, in FIGS. 25 and 26. The corresponding comparisons for the cumulative oil production and water-oil ratios are shown in FIGS. 27–30. From these

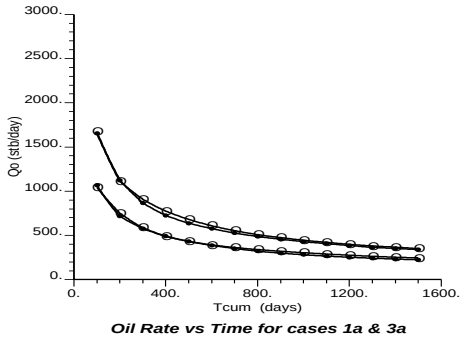

FIG. 19. *upper=3a and lower=1a.*

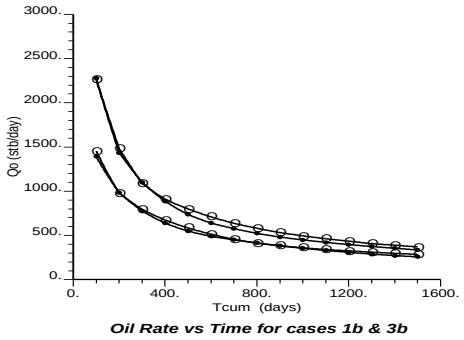

FIG. 20. *upper=3b and lower=1b.*

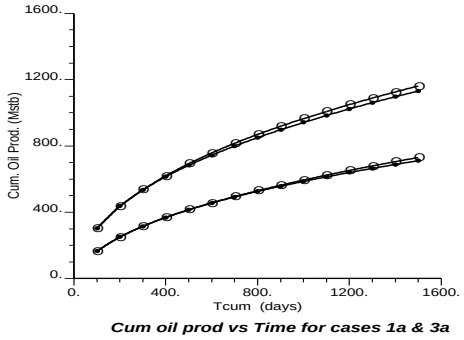

FIG. 21. *upper=3a and lower=1a.*

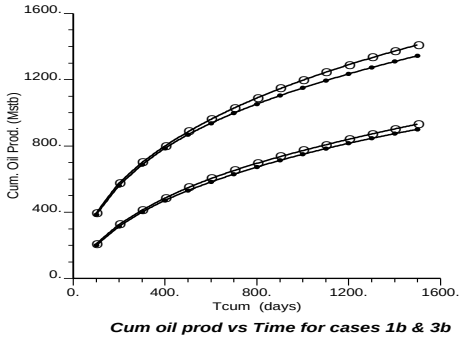

FIG. 22. *upper=3b and lower=1b.*

figures, we summarize the following observations:

- Oil production increases as the well length increases, but the production increase is limited and is not directly proportional to the length. As an example, from the comparison between Cases 1a and 1b, we see that the well length of 1b is over two times longer than that of 1a, but the cumulative oil production at 1,500 days increases only 31.5% (see FIGS. 25 and 26).
- The water coning effect decreases as the well length increases. Although the production rate in Case 1b is higher than in Case 1a, for example, the water-oil ratio in 1b is lower than in 1a. This implies that the well length increase overcomes the effect of water coning. This phenomenon can be seen from FIGS. 29 and 30, where this ratio is lower in all Cases 1b, 2b, and 3b.

6. Concluding Remarks

In this paper we have reported the recent applications of the CVFA method and presented its application to the modeling and simulation of 2D and 3D horizontal wells in petroleum reservoirs. We have developed formulas for the treatment of vertical and horizontal wells in the context of this method. Through extensive numerical experiments and comparisons with the finite difference method for benchmark flow problems, we have showed that this method can efficiently and accurately handle these wells. This lays a foundation for the modeling and simulation of these wells for other models such as the black-oil and compositional models.

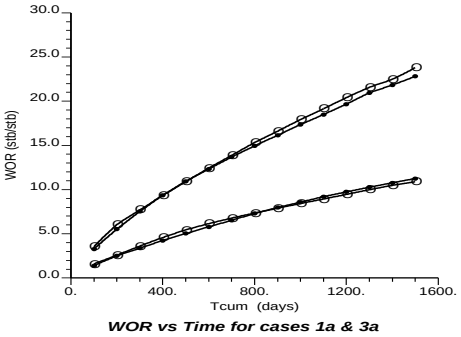

FIG. 23. *upper=3a and lower=1a.*

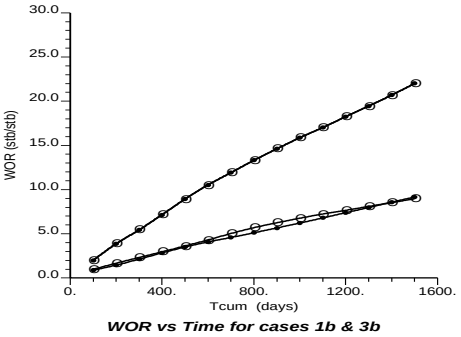

FIG. 24. *upper=3b and lower=1b.*

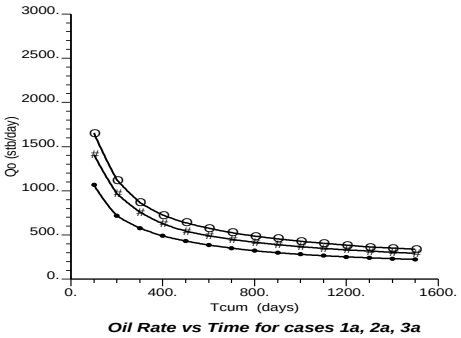

FIG. 25. •=*1a*, #=*2a, and* ∘=*3a.*

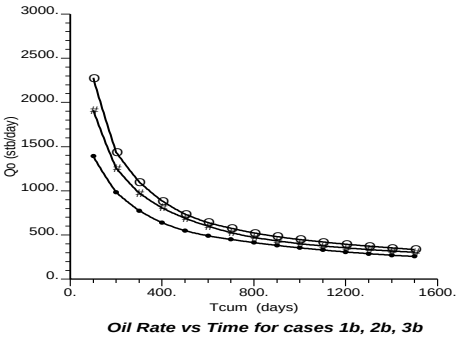

FIG. 26. •=*1b*, #=*2b, and* ∘=*3b.*

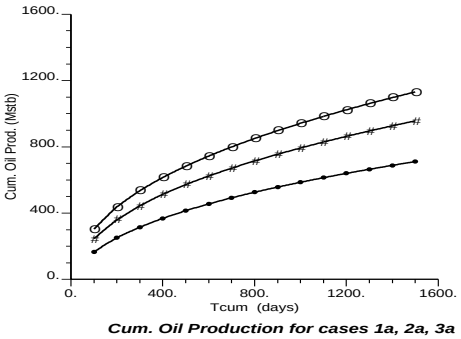

FIG. 27. •=*1a*, #=*2a, and* ∘=*3a.*

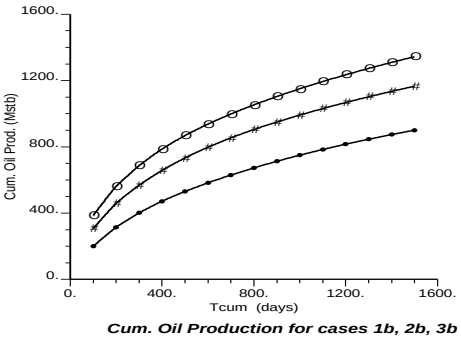

FIG. 28. •=*1b*, #=*2b, and* ∘=*3b.*

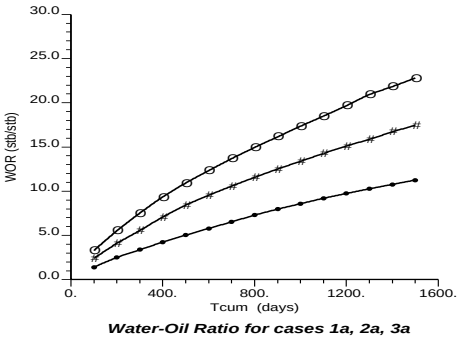

FIG. 29. •=*1a*, #=*2a*, *and* ∘=*3a*.

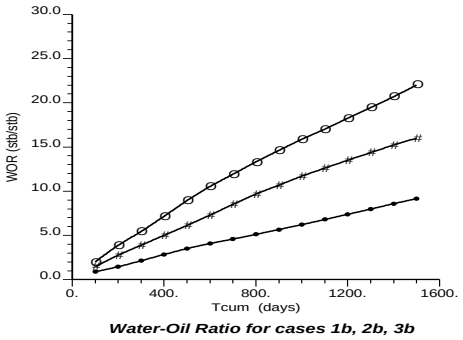

FIG. 30. •=*1b*, #=*2b*, *and* ∘=*3b*.

REFERENCES

[1] K. Aziz and A. Settari. *Petroleum Reservoir Simulation*. Applied Science Publishers Ltd, London, 1979.

[2] Z. Chen, R.E. Ewing, and Z.-C. Shi (eds.). *Numerical Treatment of Multiphase Flows in Porous Media*. Lecture Notes in Physics, Vol. 552, Springer-Verlag, Heidelberg, 2000.

[3] Z. Chen, G. Huan, and B. Li, *An improved IMPES method for two-phase flow in porous media*. Submitted to Comp. Geosciences.

[4] Z. Chen, G. Huan, and B. Li, *A benchmark calculation of 3D horizontal well simulations*. Submitted to Comp. Geosciences.

[5] P.G. Ciarlet, *The Finite Element Method for Elliptic Problems*. North-Holland, Amsterdam, 1978.

[6] D.A. Collins, L.X. Nghiem, R. Sharma, R. Agarwal, and K. Jha, *Field scale simulation of horizontal wells with hybrid grids*. SPE 21218, presented at 11th SPE Symposium on Reservoir Simulation in Anaheim, California, Feb. 17–20, 1991.

[7] R.E. Ewing (ed.), *The Mathematics of Reservoir Simulation*. SIAM, Philadelphia, 1983.

[8] L.S. Fung, L. Buchanan, and R. Sharma, *Hybrid-CVFW method for flexible grid reservoir simulation*. SPE Reservoir Engineering, 188–194, Aug. 1994.

[9] L.S. Fung, A.D. Hiebert, and L. Nghiem. *Reservoir simulation with a control volume finite element method*. SPE 21224, the 11th SPE Symposium on Reservoir Simulation, Anaheim, Feb. 17–20, 1991.

[10] Z.E. Heinemann and C.W. Brand, *Modeling reservoir geometry with irregular grids*. SPE 18412, the 10th SPE Symposium on Reservoir Simulation, Houston, Feb. 6–8, 1989.

[11] B. Heinrich, *Finite Difference Methods on Irregular Networks*. Birkhauser, Basel, Boston, Stuttgart, 1987.

[12] G. Huan, B. Li, and Z. Chen, *Applications of the control volume function approximation method to reservoir simulations*. Fluid Flows and Transport in Porous Media, Mathematical and Numerical Treatment, Z. Chen and R.E. Ewing (eds.), Contemporary Mathematics, Vol. 295, AMS, 2002, 279–292.

[13] B. Li, Z. Chen, and G. Huan, *Control volume function approximation methods for reservoir simulations*. Advances in Water Resources, to appear.

[14] L.X. Nghiem, D.A. Collins, and R. Sharma, *Seventh SPE comparative solution project: Modeling of horizontal wells in reservoir simulation*. SPE 21221, 11th SPE Symposium on Reservoir Simulation in Anaheim, California, Feb. 17–20, 1991.

[15] C.L. Palagi and K.A. Aziz, *The modeling of vertical and horizontal wells with Voronoi grid*. Paper SPE 24072, the Western Regional Meeting, Bakersfield, Mar. 30–April 1, 1992.

[16] D.W. Peaceman, *Fundamentals of Numerical Reservoir Simulation*. Elsevier, New York, 1977.

[17] D.W. Peaceman, *Interpretation of well-block pressures in numerical reservoir simulation*. SPE 6893, 52nd Annual Fall Technical Conference and Exhibition, Denver, 1977.

[18] S. Verma and K.A. Aziz, *Control volume scheme for flexible grids in reservoir simulation*. Paper SPE37999, the 1997 SPE Symposium on Reservoir Simulation, Dallas, June 8–11, 1997.